PHYSICAL REVIEW B

SOLID STATE

THIRD SERIES, VOL. 4, NO. 3 1 AUGUST 1971

Nuclear Relaxation in a Dilute *Ni*Pd Alloy

Boris Chornik*
Department of Physics, University of California, Berkeley, California
and Inorganic Materials Research Division, Lawrence Radiation Laboratory,
Berkeley, California 94720
(Received 18 March 1971)

Nuclear spin-lattice relaxation of Ni^{61} and Pd^{105} has been measured at liquid-helium temperatures in Ni metal and in a Ni 2-at.% Pd alloy. An external magnetic field of 6 kG was applied to saturate the sample, eliminating the domain walls, so that relaxation through domain-wall motion was not present. The relaxation times at 4.2 °K were 0.05 sec for Ni^{61} and 0.58 sec for Pd^{105}. The Ni relaxation time agrees well with a theoretical model based on interactions of the nuclear moments with orbital fluctuations of *d* electrons. This model and the Pd relaxation time were used to calculate a density of states at the Fermi level of 4*d* electrons on the Pd impurity. Its value turns out to be 1.0×10^{12} states (erg atom)$^{-1}$. From this value we estimated the magnetic moment localized at the Pd atom to be $0.14\mu_B$. From bulk magnetization data we conclude then that the Ni neighbors nearest to the Pd impurity have an extra moment of $0.031\mu_B$.

I. INTRODUCTION

Neutron scattering is considered the most direct tool to obtain microscopic information about the impurity magnetic state in alloys.[1-7] However, it may not yield observable results in cases of very dilute alloys, and one has to get more indirect data from other methods, e.g., the measurement of the hyperfine field at both the impurity and host nuclei (by NMR, Mössbauer effect, nuclear specific heat, etc.).[8] However, the interpretation of the results is usually difficult and somewhat ambiguous due to the presence of several contributions to the hyperfine field with opposite signs, that almost cancel. Measurement of the nuclear spin-lattice relaxation time is free from this disadvantage. In fact, the relaxation interactions are basically the same that produce the hyperfine field, but the relaxation mechanisms are additive. The most important are the well-known contact interaction with *s* conduction electrons, calculated by Korringa,[9] magnetic dipolar and orbital interaction with non-*s* electrons, discovered by Obata,[10] and core polarization, according to Yafet and Jaccarino.[11] Moriya[12] performed a calculation of the nuclear spin-lattice relaxation time in the three ferromagnetic transition metals Fe, Ni, and Co. He found that orbital interaction is dominant (by at least one order of magnitude) and that agreement with experimental results[13,14] was reasonable. In these cases, and in similar systems, interpretation of the results is very simple, since only one mechanism is dominant. From the experimental result, one can obtain the density of states of the impurity *d* electrons at the Fermi energy, therefore providing useful information about the impurity state. Such a study was made by Bancroft[15] in dilute *Ni*Cu alloys. He found a negligible density of states of Cu 3*d* electrons at the Fermi energy, and thus he inferred that the Cu impurity did not have a magnetic moment.

The present paper is a report of a nuclear spin-lattice relaxation measurement of both the Ni^{61} and the Pd^{105} nuclei in a *Ni*Pd alloy, 2-at.% concentration. The relaxation times were obtained by monitoring the recovery of the longitudinal nuclear magnetization after saturating the nuclear Zeeman levels with several rf bursts at the Larmor frequency. The spin-echo technique[16] was employed. The longitudinal nuclear magnetization is proportional to the signal that appears at a time *t* after two rf pulses separated by a fixed time *t*. An external magnetic field of 6 kG was applied to eliminate the domain walls in the sample. This is the

best way to avoid relaxation through domain-wall motion, [15] which would mask the intrinsic simple mechanisms of relaxation mentioned earlier.

An account of the experiment and results is given in Sec. II. The interpretation is developed in Sec. III, where it is found that the agreement between the experimental and theoretical relaxation times for Ni^{61} is even better than the first report[12] because of the absence of domain walls. Next, the same relaxation model is employed to derive the Pd density of states at the Fermi energy from the experimental value of the Pd relaxation time. Finally, a simple model gives the number of holes of the $4d\downarrow$ Pd levels. From there, a magnetic moment of $0.14\mu_B$ is found at the Pd site.

Our result serves to complement a recent neutron scattering experiment made by Cable and Child[7] in more concentrated Ni-Pd alloys. Both results give microscopic information on the magnetic distribution. Then it is straightforward to couple these results with the macroscopic information provided by saturation magnetization measurements[17,18] in order to get an over-all picture of the alloy magnetic properties.

II. EXPERIMENT

A. Apparatus

A block diagram of the apparatus is shown in Fig. 1. It is basically the same as used by Bancroft, [15] but the averaging procedure is more elaborate. Since the saturation method requires the measurement of the difference between the equilibrium value and the signal after a partial recovery, a good signal-to-noise ratio is necessary to obtain acceptable results. The averager served the purpose of enhancing the signal-to-noise ratio by repeating each measurement many times and integrating. It was designed as described by Samuelson and Ailion, [19] but the measurements were stored and accumulated in a multichannel analyzer instead of a single counter. Usually we measured about 15 points of the recovery curve; each measurement was stored in a separate channel of the multichannel analyzer (working in the multiscaler mode). The control unit changed the address and the recovery time automatically for each new measurement. After the 15th channel, the system went back to the first channel and started again, adding the new measurements to whatever was stored before. This configuration eliminates the effect of a slow drift of the amplifier gain, because it is shared evenly by all the averaged measurements. The accuracy improvement is remarkable in experiments that take several hours (as in our case) in comparison with the performance of a single-channel averager.

The transmitter in Fig. 1 provided the necessary

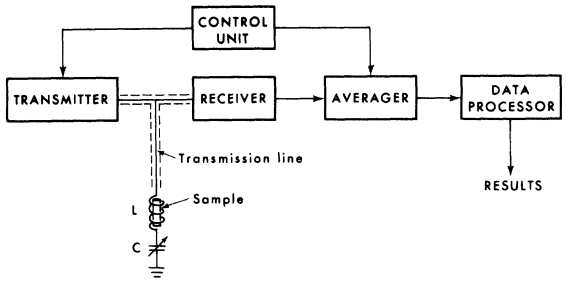

FIG. 1. Block diagram of the apparatus.

rf pulses for saturating the nuclear Zeeman levels and for monitoring the recovery to the equilibrium nuclear magnetization. It was a pulsed oscillator, Arenberg type PG-650.

The receiver consisted of a wide-band amplifier followed by a diode detector. The amplifier provided several volts of rf output in order to avoid the nonlinearity of simple diode detector circuits for signals of about 0.5 V or less. A small nonlinearity remained, however. We corrected it during the final stage of data processing with an additional subroutine in the computer program. Our design is not very common. However, we found it was easier to implement than the usual phase detector (which is linear). In a phase-coherent system, the transmitter must be a gated amplifier driven by a cw oscillator. The necessary changes in our transmitter would not have been straightforward.

B. Sample Preparation

Samples of nonannealed nickel were simply obtained from Ni sponge of 99.999% purity, supplied by Johnson-Matthey. The metal powder was mixed with N grease for electrical insulation, thus avoiding the effect of skin depth. The N grease also improved the thermal contact between the metal particles and the helium bath.

The experiment with annealed nickel was made with the same Ni sponge after a heat treatment at 600 °C for 2 h. It was performed in an Abar resistance furnace with high-vacuum facilities. The residual pressure was kept under 4×10^{-6} Torr. Alumina powder was added to avoid sintering of the nickel particles.

The Ni-Pd alloy was prepared by melting Ni and Pd sponge in an alumina crucible in the same furnace. There was a reducing atmosphere of hydrogen at the beginning to eliminate surface oxidation and facilitate the melting process. Actually the gas was a mixture of 4% H_2 and 96% He. Later, the gas was substituted by pure He. In this way we prevented H_2 from being dissolved in the liquid melt and released upon solidification, thereby pro-

ducing bubbles.

The alloy was kept at 20 °C below the melting point for 24 h in order to homogenize it. Later, the degree of homogeneity was tested with an electron-beam microprobe. The electron-beam diameter was about 1 μ. The instrument could detect variations of composition of the order of 1% or larger. It was found in our sample that the local fluctuations of composition were below the limit of sensitivity of the instrument.

The alloy was ground against a rotating disc covered with abrasive alumina paper #120. Later, the alloy particles were easily separated from the alumina particles with the help of a magnet. The last step was annealing for 2 h at 600 °C in a high vacuum to eliminate the strains produced by the cold work.

C. Experimental Results

1. *Observation of* NMR *in* Ni^{61} *and* Pd^{105}

The spin-echo technique was used. The sample temperature was 4.2 °K. Without an external magnetic field we got a resonance frequency of 28.46 MHz for Ni^{61}, both in pure Ni and in the Ni-Pd alloy, in agreement with earlier measurements[20] that used a marginal oscillator as a cw detector of NMR.

We reproduced the results of Aubrun and Khoi[21] and Bancroft[15] when an external magnetic field was applied. The resonance frequency shifted down, and for external fields higher than about 4.5 kG, the variation was linear. This shows that the hyperfine field at the Ni^{61} nucleus is negative and that the particles become magnetically saturated for external fields higher than 4.5 kG.

The argument is reinforced by the fact that the intensity of the echo went down as the magnetic field was increased. This shows that the domain walls disappeared, because the enhancement factor[22] was much bigger in the walls than in the bulk domain.

We obtained additional evidence of the change of enhancement factors when going from the zero-external-field situation to that with an external applied field. We observed the shape of the echo as a function of the amplitude and width of the rf pulses. If the turning angles were very high (much bigger than $\frac{1}{2}\pi$), the signal appeared as described by Mims.[23] For instance, if the two rf pulses had the same width, the echo was symmetrical, with a dip in the center. If the rf amplitude was reduced, so that the turning angle became of the order of $\frac{1}{2}\pi$, the echo would have a maximum in the center (as commonly happens). This center was displaced with respect to the previous case: It occurred at a time $\frac{1}{2}t_w$ later, where t_w was the rf pulse width. These changes were not seen when an external magnetic field was applied. We observed only the last case (even with the highest possible rf field), showing that the turning angle was of the order of $\frac{1}{2}\pi$ and that the enhancement factor was small.

Since the nuclei do not experience a demagnetizing field in the center of a wall, the value of the resonance frequency at zero applied field gives directly the hyperfine field. In the case of Ni^{61}, it turns out to be − 75 kOe, as calculated by Streever and Bennett[20] and using the electron-nuclear double-resonance (ENDOR) measurement of the Ni^{61} nuclear magnetic moment.[24]

The Pd resonance in the Ni-Pd alloy was found at 33.79 MHz (without an external magnetic field). This result agrees with the calculated hyperfine field of 194 kOe reported by Kontani and Itoh,[25] and obtained in a spin-echo experiment at 4.2 °K. We found that the sign of the hyperfine field is negative, as in Ni, because the resonance frequency shifted down when an external magnetic field was applied.

It was found that, after repeating the experiment several times, the signal decreased until it was completely buried in noise. This effect has not been reported before. We believe it was caused by an increase of the linewidth beyond the receiver bandwidth (about 1 MHz). This could be produced by a slight oxidation of the sample, with lattice distortions that would broaden the NMR line through electric quadrupole effects (note that Ni^{61} has a $\frac{3}{2}$ nuclear spin and Pd^{105} has a $\frac{5}{2}$ nuclear spin; the electric quadrupole moments are[26] 0.134 b for Ni^{61} and 0.8 b for Pd^{105}). The oxidation process might be enhanced by the repetition of the thermal cycle (between room temperature and liquid-helium temperature) through an increase in the number of dislocations of the sample. Hammond and Knight[27] made an experiment of nuclear quadrupole resonance in superconducting gallium particles suspended in oil or paraffin wax. They found a broadening of the resonance line and a severe loss in intensity in comparison with the same experiment performed in gallium particles mixed with quartz particles of comparable size. They attributed this change to strains produced by the contraction of the frozen oil or wax at low temperatures. The same effect in our N grease might well be part of the cause of the deterioration of the signal.

2. *Measurement of Relaxation Times*

The recovery of the magnetization, as measured by the spin-echo signal, was exponential after some time had passed. At the beginning, the relaxation was faster. This is explained in terms of diffusion of the nuclear excitation from nuclei in the center of the NMR line to nuclei at

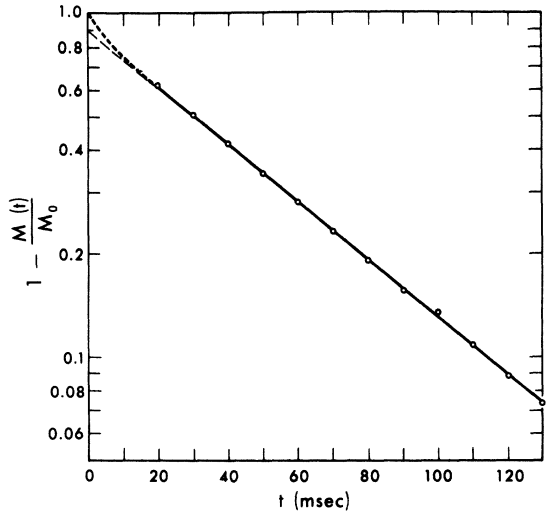

FIG. 2. Spin-lattice relaxation in Ni metal. Annealed sample. $T_1 = 52$ msec, $\beta = 0.9$, $T = 4.2\,^\circ$K.

the sides, when the latter were not excited by the rf comb.[15] There are also nuclei at the center of the NMR line that are not excited because of being too far from the surface of the sample (at a distance bigger than the rf penetration depth). We observed this effect in our experiments in the following way. We assumed a theoretical relaxation function with an additional adjustable parameter that took into account the diffusion effect. The relaxation function is

$$M(t) = M_0(1 - \beta e^{-t/T_1}) \ .$$

In this equation, M_0, β, and T_1 are unknown parameters to be calculated in a least-squares fit to the experimental data of (M, t) pairs. The results always gave $\beta < 1$, showing that there is indeed some diffusion of the spin excitation. A typical value is $\beta = 0.85$. It depended on the amplitude of the rf comb, the number of pulses, and their separation and width. The best results were obtained with a comb of 10 to 20 pulses, at the maximum transmitter voltage. The pulse separation was 1–2 msec (note that T_2 is of the order of 10 msec [28]), and the pulse width, about 10 μsec. The two rf pulses used to generate the echo had a width of 2 μsec and a separation of 500 μsec. This somewhat long time was necessary for the recovery of one of the wide-band amplifiers (Hewlett-Packard model 462-A) after being saturated by the rf pulses. However, it is still much smaller than T_2, so that the echo is not reduced. A typical relaxation curve can be seen in Fig. 2. The experiment was run under the above conditions. In Fig. 2, $[1 - M(t)/M_0]$ is plotted as a function of time in a semilogarithmic graph. The sample was pure Ni, annealed.

We expected to get a better saturation by increasing the comb length. However, we found much larger relaxation times and a nonexponential relaxation (Fig. 3, curve a). The relaxation time increased with the length of the comb. We got relaxation times more than 10 times bigger than those obtained with short combs (of about 10 to 20 pulses). In Fig. 3, curve a, the comb had 800 pulses, separated by 2 msec. For comparison, curve c is a repetition of Fig. 2 but at the same time scale as curve a. The explanation of this strange effect is simple: With long combs, the temperature of

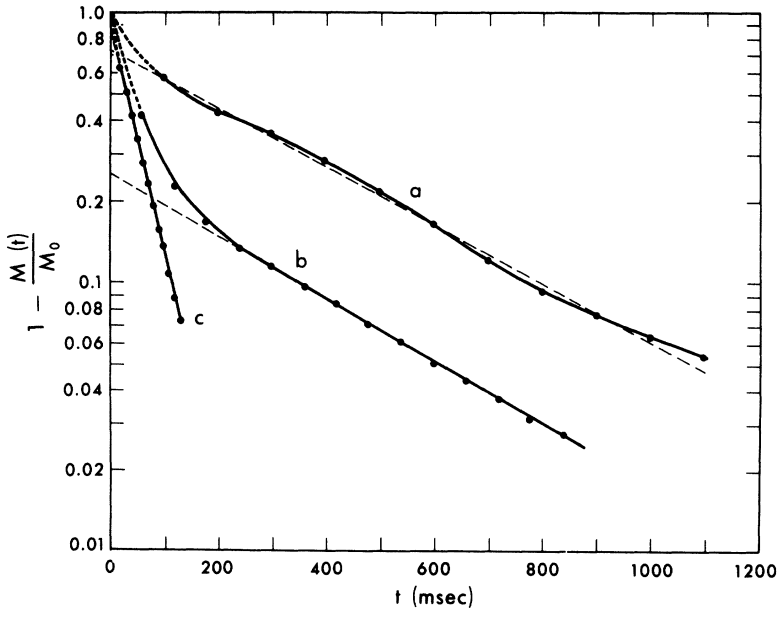

FIG. 3. Spin-lattice relaxation in different situations. Ni metal samples. $T = 4.2\,^\circ$K. (a) Long comb, produces heating of the sample. $T_1 = 401$ msec. (b) Nonannealed sample. $T_1 = 401$ msec. (b) (c) Same as in Fig. 2, but at different scale. $T_1 = 52$ msec.

the whole sample increased by eddy currents and magnetic losses. We noted also that the liquid-helium bath boiled at a much higher rate. For an additional proof, we made the following experiment: The transmitter frequency was shifted by 4 MHz (more than the linewidth), and a long comb at the new frequency was applied. The z nuclear magnetization was monitored with another transmitter in the usual way (two-pulse echo), working at the Larmor frequency. We could see a similar relaxation curve, in spite of the fact that the nuclear spins were not excited by the rf comb. This showed that the whole sample heated up and that we were monitoring the sample-bath thermal relaxation! We were able to get even longer relaxation times by increasing more the length of the rf comb. Actually case a of Fig. 3 with $T_1 = 401$ msec is an average situation. In another experiment an rf comb of 1600 pulses, separated by 1 msec, gave $T_1 = 996$ msec.

We observed also a nonexponential relaxation curve in nonannealed pure Ni samples (Fig. 3, curve b). The shape suggests broadening through strain-induced quadrupolar interactions, as found by Andrew and Turnstall, [29] Simmons, Sullivan, and Robinson, [30] and Narath. [31] The rf comb was not strong enough to saturate all the Zeeman levels: Only the central transition was excited. It is only by accident that curves a and b in Fig. 3 seem to have almost equal relaxation times. As explained before, long rf combs rendered relaxation times which varied according to the rf comb length.

After annealing the Ni sample, we obtained a purely exponential curve like c. It is not obvious why curve c has a faster relaxation time than curve b; we believe that in the latter there was an additional effect, probably surface oxidation, closely connected with the deterioration of the signal which was explained before. Besides, it was found that after repeating the experiment with the alloys, the relaxation times tended to increase. However, the pure Ni samples were much more stable. Note that in the latter the particles had a roughly spherical shape, while in the alloys the particles were rodlike (with a bigger surface area). This fact reinforces the oxidation hypothesis.

The accuracy of our results is not determined by the errors of our measurements, but by the change in sample properties. For pure Ni samples, we obtained relaxation times from 47 to 52 msec when the temperature was 4.2 °K and the external magnetic field 6 kG. As an average value, we present $T_1 = 50$ msec ± 5%.

In the *Ni*Pd alloy, 2-at.% concentration, the Ni^{61} relaxation time varied from 43 to 61 msec in the same conditions of temperature and magnetic field. Note that the average is about the same as for the pure Ni.

We shall see that the Pd relaxation time is not needed in absolute value for the calculations. Only the ratio R_{Pd}/R_{Ni} is used. Fortunately, when we measured the Pd relaxation, the Ni relaxation in the alloy was rendering about 50 msec so that the Pd value can well be considered the average. We got $T_1 = 580$ msec for Pd^{105} at 4.2 °K.

We tested the constancy of the product T_1T for the Ni^{61} relaxation in the alloy. We made two consecutive measurements at 4.2 and 2.1 °K (in order to avoid the oxidation drift). We obtained $T_1 = 61$ msec at 4.2 °K and $T_1 = 128$ msec at 2.1 °K, so that T_1T is constant within the experimental error.

III. INTERPRETATION OF RESULTS

A. Theory of Spin-Lattice Relaxation

We define a normalized relaxation rate R as

$$R = (\gamma_n^2 T_1 T)^{-1} \quad ,$$

where γ_n is the nuclear gyromagnetic ratio, T_1 is the nuclear spin-lattice relaxation time, and T is the lattice temperature. There are several contributions to R; we shall consider here the relaxation due to the interaction with the orbital electronic moment, R^{orb}, and the dipolar interaction with the electronic spin, R^{dip}. Following Obata's treatment[10] we get

$$\begin{aligned} R^{orb} &= \tfrac{4}{3}\pi\hbar^3 k_B \gamma_e^2 \langle r^{-3}\rangle^2 \textstyle\sum_\sigma [N_\sigma^d(E_F)]^2 f_\sigma (2 - \tfrac{5}{3} f_\sigma) \quad , \\ R^{dip} &= \tfrac{4}{3}\pi\hbar^3 k_B \gamma_e^2 \langle r^{-3}\rangle^2 \tfrac{1}{196}\{ 2N_\uparrow^d(E_F) N_\downarrow^d(E_F) \\ &\qquad \times (13 f_\uparrow f_\downarrow - 9 f_\uparrow - 9 f_\downarrow + 12) \\ &\qquad + \textstyle\sum_\sigma 3[N_\sigma^d(E_F)]^2 f_\sigma (2 - f_\sigma) \quad , \end{aligned} \tag{1}$$

where k_B is Boltzmann's constant, $\gamma_e = 2\mu_B/\hbar$ is the electronic gyromagnetic ratio (μ_B is the Bohr magneton), $\langle r^{-3}\rangle$ is an average at the Fermi energy, with r equal to the orbital radius, $N_\sigma^d(E_F)$ is the density of states per atom of d electrons with spin-σ only at the Fermi energy E_F, and f_σ is the fractional admixture of $d(t_{2g})$ states of spin-σ.

In addition, we have the well-known contact interaction with s electrons. The contact relaxation rate R^c derived by Korringa[9] is given by

$$R^c = \tfrac{64}{9}\pi^3\hbar^3 k_B \gamma_e^2 \langle |u_\uparrow(0)|^2\rangle_F \langle |u_\downarrow(0)|^2\rangle_F N_\uparrow^s(E_F) N_\downarrow^s(E_F)$$

where $u_\sigma(0)$ is the electronic s wave function at a nuclear site. The average $\langle |u_\sigma(0)|^2\rangle_F$ is taken at the Fermi energy. $N_\sigma^s(E_F)$ is the s density of states at the Fermi energy for spin-σ only. For the common case of a nonpolarized s band, where $N_\uparrow^s(E_F) = N_\downarrow^s = \frac{1}{2}N^s(E_F)$ and $u_\uparrow^s(0) = u_\downarrow^s(0) = u^s(0)$, we have

$$R^c = \tfrac{16}{9}\pi^3\hbar^3 k_B \gamma_e^2 \langle |u^s(0)|^2\rangle_F^2 [N^s(E_F)]^2 \quad .$$

B. Nickel Relaxation

Moriya[12] made a calculation of the relaxation rate in the case of the ferromagnetic metals Fe, Ni, and Co. He considered the above-mentioned interactions plus other (negligible) effects, like s-d exchange interaction, core polarization, and spin waves. He found that the orbital relaxation was dominant and that the agreement with experimental measurements was quite satisfactory (within a factor of 2) after correcting a mistake in the density of states.[32] Here we shall repeat the calculations in the light of better values of the various parameters needed and our new experimental results.

We obtained the average $\langle r^{-3}\rangle$ from a table of atomic wave functions (calculated by Herman and Skillman[33]) and a numerical integration. Two wave functions for nickel are tabulated, one corresponding to the $3d^9s^1$ electronic configuration and the other to $3d^8s^2$. The resultant averages differ by less than 10%, so that it is reasonably accurate to extrapolate linearly to the configuration $3d^{9.4}s^{0.6}$ which occurs in Ni metal. The result is

$$\langle r^{-3}\rangle_{\mathrm{Ni}} = 6.99 \text{ a.u.} = 4.72\times10^{25} \text{ cm}^{-3} .$$

We adopted this method of calculating $\langle r^{-3}\rangle$ considering it more direct and reliable than deriving it from hyperfine data. We assumed also that the average at the Fermi surface is the same as in the free atom, because of the localized character of the wave functions near the top of the d band (where the Fermi energy lies).

The densities of states for s and d electrons at the Fermi surface are calculated as follows: We use a total density of states $N(E_F)$ taken from an augmented-plane-wave (APW) band-structure calculation for Ni metal made by Connolly.[34] Its value is

$$N(E_F) = 1.7\times10^{12} \text{ states (erg atom)}^{-1} .$$

We assume, with Moriya, that $N_\uparrow^d(E_F) = 0$ for Ni and that

$$N(E_F) = N_\uparrow^d(E_F) + N^s(E_F) .$$

$N^s(E_F)$ is calculated from a free-electron model and the known value of the density of states of copper. The latter has only s density of states at the Fermi surface. Otherwise, its electronic structure is similar to that of Ni. An APW calculation by Burdick[35] gives

$$N_{\mathrm{Cu}}^s(E_F) = 1.4\times10^{11} \text{ states (erg atom)}^{-1} .$$

The Ni s density of states is calculated from

$$\frac{N_{\mathrm{Ni}}^s(E_F)}{N_{\mathrm{Cu}}^s(E_F)} = \left(\frac{(v_0^2 n)_{\mathrm{Ni}}}{(v_0^2 n)_{\mathrm{Cu}}}\right)^{1/3} ,$$

where v_0 is the atomic volume and n is the number of s electrons per atom (equal to 0.6 for Ni and 1 for Cu). We get finally

$$N_{\mathrm{Ni}}^s(E_F) = 1.12\times10^{11} \text{ states (erg atom)}^{-1} ,$$

$$N_{\uparrow\mathrm{Ni}}^d(E_F) = 1.59\times10^{12} \text{ states (erg atom)}^{-1} .$$

We believe the density of states derived from the band-structure calculation is more accurate for our purposes than the one calculated from specific-heat measurements. The latter is enhanced by the electron-phonon interaction and the electron-magnon interaction.[36]

Finally, the fractional admixture coefficient $f_\downarrow$ was obtained from an experiment of Bragg diffraction of polarized neutrons in Ni metal, made by Mook.[37] His result is $f_\downarrow = 0.81$.

By substitution of the numerical values, we get

$$R_{\mathrm{Ni}}^{\mathrm{orb}} = 0.62\times10^{-6}, \quad R_{\mathrm{Ni}}^{\mathrm{dip}} = 0.017\times10^{-6} .$$

Finally, we estimate the s contact relaxation indirectly, from relaxation data of copper metal. Assuming that in the latter the s contact relaxation is dominant, we have

$$\frac{R_{\mathrm{Ni}}^s}{R_{\mathrm{Cu}}^s} = \left(\frac{N_{\mathrm{Ni}}^s(E_F)}{N_{\mathrm{Cu}}^s(E_F)}\right)^2 = (0.8)^2 = 0.64 .$$

Relaxation time in Cu metal was measured by Anderson and Redfield.[38] They found $T_1T = 1.27$ for Cu; hence,

$$R_{\mathrm{Ni}}^s = 0.0102\times10^{-6} .$$

Thus the s contact relaxation in Ni is 1.3% of the orbital relaxation. Adding the three effects, we get

$$R_{\mathrm{Ni}} = R_{\mathrm{Ni}}^{\mathrm{orb}} + R_{\mathrm{Ni}}^{\mathrm{dip}} + R_{\mathrm{Ni}}^s = 0.65\times10^{-6} .$$

So far, we have essentially repeated Moriya's calculation, but with new values for $\langle r^{-3}\rangle$ and $N_\uparrow^d(E_F)$. The first parameter is bigger and the second smaller than those used by Moriya. Our final result is about 20% smaller. On the other hand, our experimental relaxation time is longer than the one available at the time of Moriya's paper. The 6-kG magnetic field effectively swept away the domain walls, thereby eliminating the relaxation produced by domain-wall motion.[14] From $T_1 = 0.05$ sec and $T = 4.2\,^\circ$K, we get

$$R_{\mathrm{Ni}}(\mathrm{expt}) = 0.84\times10^{-6} .$$

Agreement between theory and experiment are well within the estimated experimental error and the uncertainties in the theoretical calculation of $N_\uparrow^d(E_F)$ and $\langle r^{-3}\rangle$. This supports the interpretation of the measured Ni relaxation time as caused mainly by the orbital interaction, excluding the effect of domain-wall motion.

C. Palladium Relaxation

Since the orbital interaction is well established as the dominant mechanism of relaxation, we can use the experimental value of the Pd relaxation time to obtain the $4d$ density of states at the Fermi level of the Pd impurity. From formula (1), we get

$$\frac{R_{\mathrm{Pd}}^{\mathrm{orb}}}{R_{\mathrm{Ni}}^{\mathrm{orb}}} = \left(\frac{\langle r^{-3}\rangle_{\mathrm{Pd}}}{\langle r^{-3}\rangle_{\mathrm{Ni}}}\right)^2 \frac{\{[N_{\uparrow\mathrm{Pd}}^{4d}(E_F)]^2 + [N_{\uparrow\mathrm{Pd}}^{4d}(E_F)]^2\}}{[N_{\uparrow\mathrm{Ni}}^{3d}(E_F)]^2} \ .$$

Here we assumed that the f coefficients for the Pd impurity are equal to those of Ni. This assumption can be removed without too much change in the final results, since the relaxation rate does not depend very strongly on f.

The average $\langle r^{-3}\rangle$ for $4d$ orbitals in Pd is calculated in the same way as the one for $3d$ orbitals in Ni. In this case, we just use the listed table for the $4d^{10}$ configuration. We get

$$\langle r^{-3}\rangle_{\mathrm{Pd}} = 7.65 \text{ a.u.} = 5.16\times10^{25} \text{ cm}^{-3} \ .$$

From the experimental result, $T_1 = 0.58$ sec at $4.2\,^{\circ}$K for Pd, we get

$$R_{\mathrm{Pd}}^{\mathrm{orb}}(\mathrm{expt}) = 0.34\times10^{-6} \ .$$

Hence,

$$\{[N_{\uparrow\mathrm{Pd}}^{4d}(E_F)]^2 + [N_{\uparrow\mathrm{Pd}}^{4d}(E_F)]^2\}^{1/2}$$

$$= \frac{4.72}{5.16}\times1.68\times10^{12}\left(\frac{0.34}{0.84}\right)^{1/2}$$

$$= 0.99\times10^{12} \text{ states (erg atom)}^{-1} \ .$$

D. Description of Impurity State

The problem of finding the impurity levels has not yet been solved quantitatively. In the *Ni*Pd case, all we can do is to gather several experimental facts (including our measurements) and propose a structure that would agree reasonably well with all of them. We are interested in the shape of the Pd levels and their position with respect to the Fermi energy. Figure 4 shows several possibilities. The spin-up and spin-down states are drawn separately to take into account a possible splitting. In all cases, the ordinates represent the electron energy with respect to the Fermi energy and the abscissae are the impurity densities of states. The area under each sub-band corresponds to five electrons per atom. States are filled up to the Fermi energy (shadowed areas).

Straightforward considerations allow us to neglect immediately most cases. Because of charge neutrality within the impurity cell, we can eliminate cases f, g, h, and i. Because of the ferromagnetic state of the alloy, we may assume there is a molecular field acting on the Pd $4d$ levels from the exchange interaction between $3d$ electrons of Ni and $4d$ electrons of Pd. Therefore, we exclude cases a and d. Our measurement of the Pd relaxation time tells that there is a sizable density of states of the impurity level at the Fermi energy. Because of this experimental fact, we eliminate case c. The only remaining possibilities are b and e. Note that case b is similar to the $3d$ band in nickel metal. It is interesting to estimate for this model the number of holes in the $4d\downarrow$ levels. Let us assume that the density-of-states–vs–energy curve has a parabolic shape near the Fermi energy, or $E \sim [N(E)]^2$, where E is the energy measured from the intercept of the curve with the E axis, so that $N(0) = 0$. In this approximation, the number of holes n_h is given by

$$n_h \sim [N(E_F)]^3 \ .$$

We obtain a rough estimate of n_h for the Pd impurity by assuming that the Ni $3d$ band has the same shape and using the known values of $N(E_F)$ and n_h for Ni. The latter comes from measurements of the g factor[18] equal to 2.18 and the saturation magnetization,[39] which give $(n_h)_{\mathrm{Ni}} = 0.565$ holes/atom:

$$\frac{(n_h)_{\mathrm{Pd}}}{(n_h)_{\mathrm{Ni}}} = \frac{[N_{\mathrm{Pd}}(E_F)]^3}{[N_{\mathrm{Ni}}(E_F)]^3} \ , \quad (n_h)_{\mathrm{Pd}} = 0.11 \ \frac{\text{holes}}{\text{atom}} \ .$$

In order to examine the possibility of case e, let us estimate the splitting of the $4d$ sub-bands of the impurity. We may assume in a first approximation it is of the same order of the splitting of the $3d$ sub-bands of Ni. The latter is not known accurately. Connolly[34] found a 0.9-eV splitting in an APW calculation of the band structure. Zornberg[40] obtained a smaller splitting between

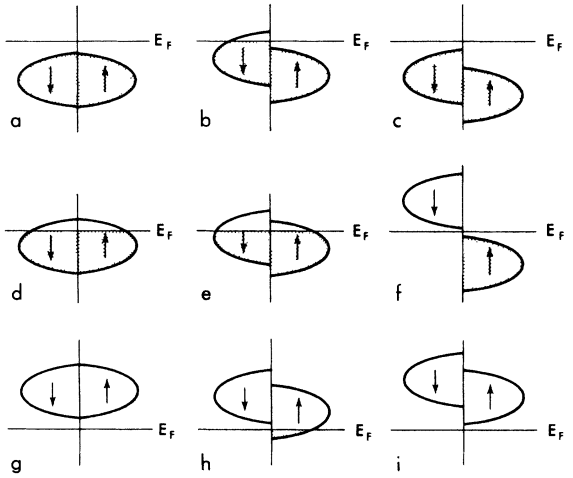

FIG. 4. Density of states vs energy for the impurity levels. Spin-up and spin-down are separated. Nine different possibilities are considered.

0.4 and 0.6 eV, from optical-spectra data. Phillips[41] tabulates the results of many authors, ranging from 0.3 to 1.7 eV, and finally estimates a splitting of 0.5 ± 0.1 eV in coincidence with Zornberg.

A 0.5-eV splitting would eliminate immediately case e of Fig. 4 because the density of states at the Fermi surface would be higher than the Ni $3d$ density of states. Our measurements show just the opposite result: $N_{\mathrm{Pd}}^{4d} < N_{\mathrm{Ni}}^{3d}$.

On choosing model b, there are two important consequences: (i) a density of states that agrees with our measurements of spin-lattice relaxation time, and (ii) a small magnetic moment localized at the impurity. Its value is obtained from the calculated number of holes, $n_h = 0.11$, and the measured value of the orbital contribution. Fischer, Herr, and Meyer[18] obtained for Pd a g factor of 2.58 in Ni-Pd alloys. Hence,

$$\mu_{\mathrm{Pd}} = \tfrac{1}{2}(2.58) \times 0.11\,\mu_B = 0.14\,\mu_B \ .$$

We have to emphasize now that this result is the consequence of a simple model that assumes equal shape for the $4d$ impurity levels and the $3d$ Ni band.

E. Discussion

Here we would like to compare the prediction of a moment of $0.14\mu_B$ localized at the Pd impurity (from our model) with the results of other experiments.

1. *Hyperfine Field at* Pd *Nucleus*

In ferromagnetic alloys the two dominant contributions to the hyperfine field are[8] contact interaction by conduction electrons and contact interaction by s core electrons. Both are polarized by s-d exchange. The core polarization is important if there is a magnetic moment at the impurity site. Shirley, Rosenblum, and Matthias[42] calculated a conduction-electron contribution of -79 kOe for the Pd impurity in Ni. Since the total hyperfine field is -194 kOe, there is an additional -115-kOe field that they attributed to s core polarization. From there, a magnetic moment of $0.3\mu_B$ at the Pd site was obtained.

Note that calculations of hyperfine fields use the exchange-polarized Hartree-Fock method,[8] where the wave functions of opposite spin direction are evaluated separately. The net spin density results in a difference between the two charge densities of opposite spins. The difference turns out to be much smaller than each term, so that there may be a large relative error. That is the reason why the hyperfine-field prediction of the Pd magnetic moment cannot be considered more accurate than the one derived from our measurement of the Pd relaxation time. We do not see, therefore, a substantial disagreement between both results.

2. *Measurement of Magnetic Moment by Neutron Scattering*

Cable and Child[7] performed experiments of Bragg and diffuse scattering of polarized neutrons in four Ni-Pd alloys. The Pd concentration ranged from 25 to 92 at.%. They found that both the Pd and the Ni magnetic moments increased with Pd concentration in the Ni-rich region. Their values are, for Pd, $(0.00 \pm 0.03)\mu_B$ and $(0.17 \pm 0.01)\mu_B$ in the 25-at.% alloy and the 50-at.% alloy, respectively. For Ni, they are $(0.81 \pm 0.01)\mu_B$ and $(1.02 \pm 0.01)\mu_B$ in the same alloys. From the observed trend and the measured values, they predicted that the Pd moment would be zero for very dilute alloys. Unfortunately, neutron scattering does not yield observable results for Ni-rich very dilute alloys, and one has to rely on an extrapolation (as Cable and Child did) or use an indirect method of obtaining the magnetic moment (as in our experiment). The different results do not show a fundamental disagreement, but they rather indicate the domain where each method gives reliable results. Even at 25-at.% concentration, the neutron diffuse scattering measurement requires a sizable correction for multiple Bragg scattering, so that the calculated Pd moment for the 25-at.% alloy is less reliable than the one for the more concentrated alloys.[43]

3. *Magnetization vs Concentration for* Ni-Pd *Alloys*

Crangle and Scott[17] and Fischer, Herr, and Meyer[18] measured the average magnetic moment per atom, M_{av}, as a function of concentration. They found that M_{av} decreases linearly with Pd concentration from 0 up to 50% Pd. In this region of concentration, the following relation is followed very closely:

$$M_{\mathrm{av}} = (0.616 - 0.11c)\mu_B \ ,$$

where c is the Pd concentration. For $c > 0.5$, M_{av} drops faster and vanishes at about $c \approx 0.98$.

It was suggested that for $c < 0.5$, the Ni moment remains constant ($0.616\mu_B$) and each Pd atom contributes with $0.506\mu_B$. However, the Pd contribution does not need to be localized at the Pd atom. It can be shared by the neighbor Ni atoms, as proposed by Cable and Child.[7] Analogously, a magnetic moment disturbance on the impurity neighbors has been found by neutron diffuse scattering in other alloys.[3,4,6]

Let us assume the Pd impurity has a $0.14\mu_B$ moment (as proposed before) and only the nearest neighbors have a bigger moment, so that the total Pd contribution is $0.506\mu_B$. Thus the 12 nearest neighbors have an extra moment of $(0.506 - 0.14)\mu_B$

$= 0.366\mu_B$ and each one of them has an extra moment of $0.031\mu_B$, or a $0.647\mu_B$ total moment.

We think the explanation of the enhanced Ni moment is part of the whole problem of the Pd states in Ni. Stearns[44] postulated that there is an antiferromagnetic indirect interaction via *s* conduction electrons, to explain the Mössbauer spectra of alloys of iron with different impurities. If the same effect occurs in the *Ni*Pd alloys, then the lack of moment on the Pd atom would increase the moment on the Ni neighbors. We present now another qualitative explanation based on screening effects. It is known that in free Pd atoms the 4*d* orbitals have a lower energy than 3*d* orbitals in Ni (see, for example, Herman and Skillman's calculations[33]). The origin of this fact is that the 4*d* orbitals in Pd have a sizable density in regions of space where the extra nuclear charge has not been screened by the inner electronic shells. Therefore, the 4*d* states of Pd in the alloy are more filled than the 3*d* states of Ni because of the extra nuclear charge of Pd, in agreement with our previous conclusions. There is an extra negative charge of $0.565 - 0.11 = 0.45$ electrons per atom, to be screened by *s* conduction electrons and 3*d* electrons from the Ni nearest neighbors. In other words, 3*d* and 4*s* electrons from the Ni nearest neighbors move in to partially fill the Pd 4*d* states. Since only the spin-down sub-band has a large density of states at the Fermi energy, the screening will be done by $3d\downarrow$ electrons, thereby increasing the magnetic moment of the Ni nearest neighbors.

IV. SUMMARY AND CONCLUSIONS

We detected the NMR and measured the spin-lattice relaxation time of Ni^{61} and Pd^{105} in a *Ni*Pd alloy, 2-at.% concentration. The Ni^{61} relaxation time agrees with a theoretical model in which the dominant mechanism of relaxation is an interaction with orbital fluctuations of *d* electrons. Assuming that the same mechanism applies to the Pd^{105} relaxation, we derived the value for the density of states at the Fermi surface of the 4*d* Pd levels. From this, we inferred a magnetic moment at the Pd impurity, and estimated its value to be $0.14\mu_B$. The accuracy of this result is limited by the assumption that the 4*d* Pd levels have a density-of-states curve of the same shape as that of the 3*d* Ni levels. We adopted this assumption for lack of anything better. This result does not disagree substantially with measurements of the hyperfine field[42] and experiments using diffuse neutron scattering.[7]

Next, we presented a model of magnetic moment distribution around the impurity, made to agree with bulk magnetization measurements, as first suggested by Cable and Child.[7] Only nearest neighbors are perturbed with respect to the pure host. In order to test this model, it would be interesting to observe the structure of the NMR Ni^{61} line in the alloy. One would expect a satellite line because of the different environment of the Ni^{61} nearest neighbors to the Pd impurity. A similar situation was found in a *Co*Ni alloy by La-Force, Ravitz, and Day,[45] and Riedi and Scurlock.[46] We can estimate the displacement of the satellite line from the calculations of hyperfine fields by Shirley, Rosenblum, and Matthias.[42] Suppose there is only a change of the core-polarization field produced by the change of the magnetic moment. In Ni metal, the calculated core-polarization field is -50 kG. Hence, in the nearest neighbors to the Pd impurity, we would have a change in the hyperfine field H_{hfs},

$$\Delta H_{hfs} = -50 \times 0.031/0.616 = -2.5 \text{ kG}.$$

That means an increase of frequency of 0.95 MHz, which can be easily detected.

Our work is part of a wide-range project of study of different impurities in Ni. The first case was a *Ni*Cu alloy, studied by Bancroft,[15] who found that there was no magnetic moment at the Cu site. The Cu impurity has very similar electron levels to Ni and differs only in one unit of valence. In our case, Pd has the same valence as Ni, but differs only in atomic size. We can see that Cu and Pd are two qualitatively different cases, and that other impurities in Ni would have similar behaviors, approaching one of the two cases or something intermediate. In particular, we are planning to work with the following alloys: *Ni*Pt, *Ni*Ir, and *Ni*Rh.

ACKNOWLEDGMENTS

I would like to thank Professor Alan M. Portis for suggesting the subject of this research work and for his invaluable help during its completion. I am indebted to Professor Leo M. Falicov for very illuminating discussions that led to the interpretation of the experimental results. This work was done under the auspices of the University of Chile—University of California Exchange Program, with support from the U. S. Atomic Energy Commission through the Inorganic Materials Research Division of the Lawrence Radiation Laboratory.

*Present address: Departamento de Física, Facultad de Ciencias Físicas y Matemáticas, Universidad de Chile, Casilla 5487, Santiago, Chile.

[1]G. G. Low and M. F. Collins, J. Appl. Phys. 34, 1195 (1963).

[2]W. Marshall, J. Phys. C 1, 88 (1968).

[3]M. F. Collins and G. G. Low, Proc. Phys. Soc. (London) 86, 535 (1965).

[4]J. B. Comly, T. M. Holden, and G. G. Low, J. Phys. C 1, 458 (1968).
[5]G. G. Low, J. Appl. Phys. 39, 1174 (1968).
[6]J. W. Cable, J. O. Wollan, and H. R. Child, Phys. Rev. Letters 22, 1256 (1969).
[7]J. W. Cable and H. R. Child, Phys. Rev. B1, 3809 (1970).
[8]A. J. Freeman and R. E. Watson, in *Magnetism*, edited by G. T. Rado and M. Suhl (Academic, New York, 1965), Vol. 2-A.
[9]J. Korringa, Physica 16, 601 (1950).
[10]Y. Obata, J. Phys. Soc. Japan 18, 1020 (1963).
[11]Y. Yafet and V. Jaccarino, Phys. Rev. 133, A1630 (1964).
[12]T. Moriya, J. Phys. Soc. Japan 19, 681 (1964).
[13]M. Weger, E. L. Hahn, and A. M. Portis, J. Appl. Phys. 32, 124S (1961).
[14]M. Weger, Phys. Rev. 128, 1505 (1962).
[15]M. H. Bancroft, Phys. Rev. B2, 182 (1970).
[16]E. L. Hahn, Phys. Rev. 80, 580 (1950).
[17]J. Crangle and W. R. Scott, J. Appl. Phys. 36, 921 (1965).
[18]G. Fischer, A. Herr, and A. J. P. Meyer, J. Appl. Phys. 39, 545 (1968).
[19]G. L. Samuelson and D. C. Allion, Rev. Sci. Instr. 40, 676 (1969).
[20]R. L. Streever and L. H. Bennett, Phys. Rev. 131, 2000 (1963).
[21]J. N. Aubrun and L. D. Khoi, Compt. Rend. 263 B249 (1966).
[22]A. C. Gossard and A. M. Portis, J. Appl. Phys. Suppl. 31, 205 (1960).
[23]W. B. Mims, Phys. Rev. 141, 499 (1966).
[24]P. R. Locher and S. Geshwind, Phys. Rev. Letters 11, 333 (1963).
[25]M. Kontani and J. Itoh, J. Phys. Soc. Japan 22, 345 (1966).
[26]V. S. Shirley, in *Hyperfine Structure and Nuclear Radiations*, edited by E. Matthias and D. A. Shirley (North-Holland, Amsterdam, 1968).
[27]R. H. Hammond and W. D. Knight, Phys. Rev. 120, 762 (1960).
[28]M. H. Bancroft, UCRL Report No. UCRL-18461, 1968 (unpublished).
[29]E. R. Andrew and D. P. Tunstall, Proc. Phys. Soc. (London) 78, 1 (1961).
[30]W. W. Simmons, W. J. O'Sullivan, and W. A. Robinson, Phys. Rev. 127, 1168 (1962).
[31]A. Narath, Phys. Rev. 162, 320 (1967).
[32]R. E. Waldstedt, V. Jaccarino, and N. Kaplan, J. Phys. Soc. Japan 21, 1843 (1966).
[33]F. Herman and S. Skillman, *Atomic Structure Calculations* (Prentice-Hall, Englewood Cliffs, N. J., 1963).
[34]J. W. D. Connolly, Phys. Rev. 159, 415 (1967).
[35]G. A. Burdick, Phys. Rev. 129, 138 (1963).
[36]L. C. Davis and S. H. Liu, Phys. Rev. 163, 503 (1967).
[37]H. A. Mook, Phys. Rev. 148, 495 (1966).
[38]A. G. Anderson and A. G. Redfield, Phys. Rev. 116, 583 (1959).
[39]H. Danan, A. Herr, and A. J. P. Meyer, J. Appl. Phys. 39, 669 (1968).
[40]E. I. Zornberg (unpublished).
[41]J. C. Phillips, J. Appl. Phys. 39, 755 (1968).
[42]D. A. Shirley, S. S. Rosenblum, and E. Matthias, Phys. Rev. 170, 363 (1968).
[43]J. W. Cable (private communication).
[44]M. B. Stearns, J. Appl. Phys. 36, 913 (1965).
[45]R. C. LaForce, S. F. Ravitz, and G. F. Day, Phys. Rev. Letters 6, 226 (1961).
[46]P. C. Riedi and R. G. Scurlock, J. Appl. Phys. 39, 124 (1968).

PHYSICAL REVIEW B VOLUME 4, NUMBER 3 1 AUGUST 1971

Fluorescent Spectra of Sm^{2+} in KCl. I. Evidence for C_{2v} Site-Symmetry Origin of $^7F_3$ Lines*

R. E. Bradbury and E. Y. Wong
Department of Physics, University of California, Los Angeles, California 90024
(Received 3 August 1970)

In a recent publication Fong claimed a C_s site-symmetry origin for certain lines in the $^7F_3$ and $^7F_4$ regions (corresponding to transitions $^5D_0 \rightarrow {}^7F_3$, $^7F_4$) of the fluorescent spectrum of Sm^{2+} in KCl. The present authors point out that the evidence cited for the lines in the $^7F_4$ regions (8128.0 and 8122.5 Å) is inconclusive and present experimental proof that both his data as presented and the curves fitted to the data for the lines at 7693.5 and 7694.5 Å are incorrect. Arguments are also presented that the best assignment of site-symmetry origin is C_{2v}.

I. INTRODUCTION

The spectrum of Sm^{2+} doped in KCl was first studied by Bron and co-workers.[1-3] The Sm^{2+} ion goes into a K^+ site in the cubic lattice, but different symmetries may be induced at the Sm^{2+} site, depending on the location of the K^+ vacancy necessary to compensate for the excess charge on the Sm^{2+} ion. Bron and co-workers' assumption that most of the Sm^{2+} ions are in C_{2v} symmetry with the K^+ vacancy at the 110 position was substantiated by a very complete explanation of the absorption and fluorescence spectra. Fong and Wong, having some doubts about the crystal field analysis, later used the Zeeman

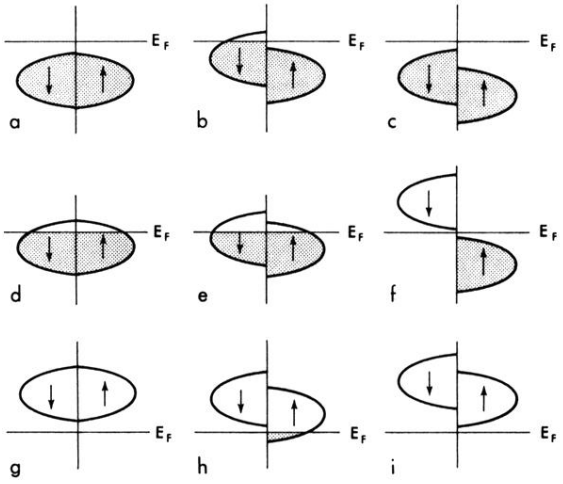

FIG. 4. Density of states vs energy for the impurity levels. Spin-up and spin-down are separated. Nine different possibilities are considered.